First Operation of a Storage-Ring Free-Electron Laser

M. Billardon,[a] P. Elleaume,[b] J. M. Ortega,[a] C. Bazin, M. Bergher, M. Velghe,[c] and Y. Petroff
Laboratoire pour l'Utilisation du Rayonnement Electromagnétique, Université de Paris-Sud, F-91405 Orsay, France

and

D. A. G. Deacon,[d] K. E. Robinson, and J. M. J. Madey
High Energy Physics Laboratory, Stanford University, Stanford, California 94305
(Received 1 August 1983)

A storage-ring free-electron laser oscillator has been operated above threshold at a visible wavelength $\lambda \simeq 6500$ Å.

PACS numbers: 42.60.-v

A free-electron laser (FEL) generates stimulated radiation by interaction of relativistic free electrons with a spatially oscillating magnetic field (undulator). The wavelength, λ, of the stimulated radiation emitted along the axis is given approximately by (in SI units)

$$\lambda = \frac{\lambda_0}{2\gamma^2}\left(1+\frac{K^2}{2}\right), \quad K = \frac{eB_0\lambda_0}{2\pi mc}, \tag{1}$$

where e and m are the electron charge and mass, c is the speed of light in vacuum, B_0 and λ_0 are the undulator peak magnetic field and period, and γ is the total electron energy divided by mc^2. The first operation[1] of a FEL has been demonstrated by the Stanford group at $\lambda = 3.4$ μm using 43-MeV electrons produced by a linear accelerator. In any practical design, $\lambda_0 \gtrsim 3$ cm; therefore it is obvious from Eq. (1) that operation of a visible or ultraviolet FEL needs a high-energy accelerator of $\gamma mc^2 \gtrsim 100$ MeV. In this energy range, storage rings are superior to linear accelerators in terms of electron density, energy spread, and emittance, thus resulting in a higher optical gain. In this Letter, we report the first operation of a storage-ring free-electron laser oscillator above threshold at $\lambda \simeq 6500$ Å.

We have used the Orsay storage ring ACO, an "older" machine, first operated in 1965. Its characteristics for this experiment are given in Table I. A permanent magnetic undulator of 17 periods optimized for electrons of 240-MeV energy has been built.[2] However, the limited straight-section length (1.3 m) available on ACO left us with a low gain of a few parts in 10^{-4} per pass in earlier work.[3] Laser oscillation was therefore impossible. Now, a gain enhancement by a factor 2 to 7 has been achieved by modifying the undulator into an optical klystron[4] (OK). This was done by replacing the three central periods by a three-pole wiggler (dispersive section). This section strongly enhances the bunching originating from electron and radiation interaction in the first undulator section and therefore gives a larger energy exchange between electrons and radiation field in the second undulator section.[4]

Mirror reflectivity degradation has been observed[3] at 240-MeV electron energy. This degradation is mainly due to the uv part of the spontaneous emission from the klystron. This problem was overcome by operating the OK at minimum K (by increasing the magnetic gap) to minimize the harmonic content of the spontaneous emission, and the storage ring at the minimum electron energy to also diminish the flux. It is

TABLE I. ACO characteristics in the FEL experiment.

Energy	160 – 166 MeV
Circumference	22 m
Bunch to bunch distance	11 m
Electron beam current for oscillation	16 to 100 mA
rms bunch length σ_l	0.5 to 1 ns
rms bunch transverse dimensions σ_x, σ_y	0.3 to 0.5 mm
rms angular spread σ_x', σ_y'	0.1 to 0.2 mrad
rms relative energy spread	$(0.9 \text{ to } 1.3) \times 10^{-3}$
Electron beam lifetime	60 to 90 min

TABLE II. Optical cavity characteristics.

Length	5.5 m
Mirror radius of curvature	3 m
Rayleigh range	1 m
Wavelength of maximum Q	620 to 680 nm
Average mirror reflectivity at 6328 Å	99.965%
Round trip cavity losses at 6328 Å	7×10^{-4}
Mirror transmission	3×10^{-5}

possible by decreasing both K and γ to keep λ constant around 6500 Å which gives the maximum reflectivity for the mirrors used in this experiment. The OK was finally operated at $K=1.1$ to 1.2 with a dispersive section characterized by[5] $N_d \simeq 95$ where N_d is the number of laser optical wavelengths passing over an electron in the dispersive section. The optical cavity characteristics are given in Table II.

Laser oscillation was obtained after a careful alignment of the electron beam on the cavity axis (within 0.1 mm all along the 1.3-m OK length) and maximization of emission as a function of the storage-ring radio-frequency cavity voltage and the optical-cavity length. Laser operation requires very precise synchronism between light-pulse reflections and electron-bunch revolution

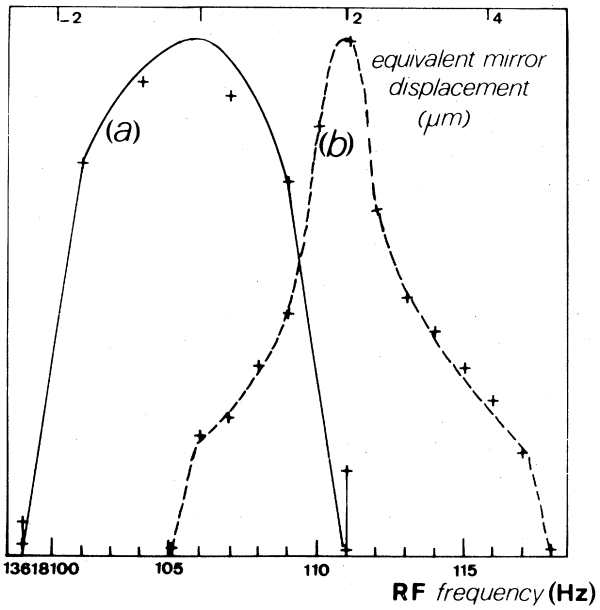

FIG. 1. Normalized laser power as a function of rf frequency and equivalent mirror displacement. Curve a is recorded close to the maximum gain/loss ratio and curve b close to the laser threshold. The shift between the two curves is probably due to some slight cavity-length drift.

frequency. To avoid backlash and mirror misalignment, fine tuning of the cavity length was performed by slightly changing the frequency instead of translating the mirrors. Laser oscillation lasted typically 1 h after each electron injection.

Figure 1 shows two "detuning curves" of laser power (normalized to the maximum) versus frequency variation and equivalent mirror displacement. Curve (a) has a 3.4 μm full width at half maximum of equivalent mirror displacement; curve (b), as recorded much closer to laser threshold, has only a 1.6 μm full width at half maximum. The shift in displacement between curves (a) and (b) is probably due to some slow cavity length drift [e.g., a temperature drift of (0.02 °C)/(30 min) would be sufficient]. In this experiment, the gain was not proportional to the electron current, mainly because of the anomalous bunch lengthening and energy spreading at high current; these effects make the gain versus ring current reach a maximum and then decrease. One consequence of this is that the ratio of gain to cavity losses always remained just above 1 during laser operation. Wider detuning curves are expected for higher gain/loss ratios.

Figure 2 presents the horizontal and vertical transverse profiles of the laser output. They are in a very good agreement with the expected cavity TEM_{00} profile. The slight discrepancies might arise from some residual instability of the laser too close to threshold or nonuniform mirror reflectivity.

Figure 3 shows the laser time structure in a 200-ms total time scale. Quasirandom peaks appear in curve (a). Curve (b) is obtained by increasing the detector sensitivity and shows some substructure in the peaks. Although not seen in Fig. 3, each subpeak is also usually more or less modulated at 13 kHz, very close to the theoretical rf synchrotron frequency, and also shows a typical rise time around 200 μs corresponding to a gain minus cavity losses of 2×10^{-4}/pass. It should be noted that this time structure highly de-

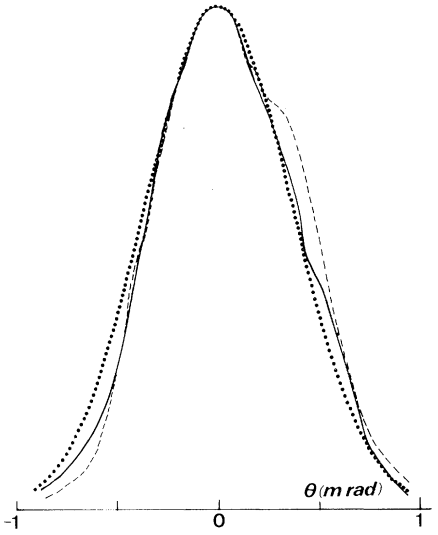

FIG. 2. Experimental laser horizontal (solid curve), vertical (dashed curve) transverse profiles, and the calculated (dotted curve) cavity TEM_{00} profile.

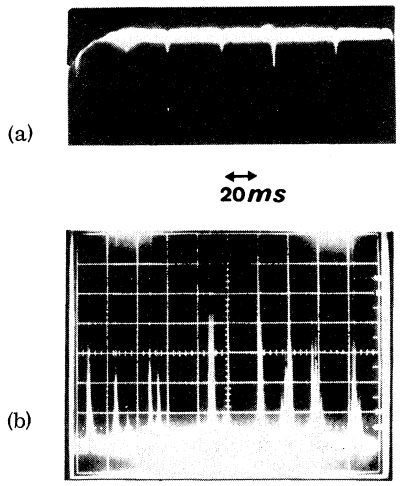

FIG. 3. Laser time structure over a 200-ms interval. Curve *b* is recorded in the same condition as *a*, but with a higher detector sensitivity.

pends on how far the laser is from threshold. Quasiperiodic peaks have sometimes been seen near a 40-Hz frequency. And the laser variation also reproduces the pulsed 27.2-MHz structure of the electron beam.

Figure 4 presents two spectra: (a) is recorded without amplification (optical cavity completely detuned) and (b) is recorded at laser operation (cavity tuned). For case (b), the laser oscillates at three wavelengths, with the strongly dominant one being at $\lambda = 6476$ Å; each wavelength is located at a maximum of the gain versus wavelength curve.[5] Smaller gain/loss ratios would restrict the number of laser wavelengths to two or one. Typical laser lines are Gaussian if averaged over a long time scale of $\gtrsim 1$ sec, with 2 to 4 Å full width at half maximum. Figure 4 also shows an enlargement of the main laser-line spectrum recorded by using a one-dimensional charge-coupled-device (CCD) detector instead of the usual monochromator exit slit. The aperture time is 3 ms. Each narrow square peak in this curve is recorded on only one CCD element and corresponds to a 0.3 Å spectral width which is of the same order as the monochromator resolution. We conclude that there is a residual inhomogeneous contribution to the laser linewidth probably connected with the long-time-scale laser-pulse structure (see Fig. 4). The central wavelength of any line is always equal to the wavelength of maximum emission of spontaneous emission with the cavity completely detuned (no amplification) plus 0.15 of the wavelength interfringe distance (see Fig. 4) instead of 0.25 as predicted from Madey's theorem.[6] This discrepancy is probably due to the transverse multimode content of the spontaneous emission stored in the cavity; laser operation is only achieved on the TEM_{00} mode. Laser tunability was obtained between 640 and 655 nm by changing the magnetic gap [equivalent to a change of K in Eq. (1)]. The range of tunability is in fact limited for the moment by the mirror reflectivity.

A typical 75-μW average output power has been recorded at 50-mA current of 166-MeV electrons. This corresponds to a typical 60-mW output peak

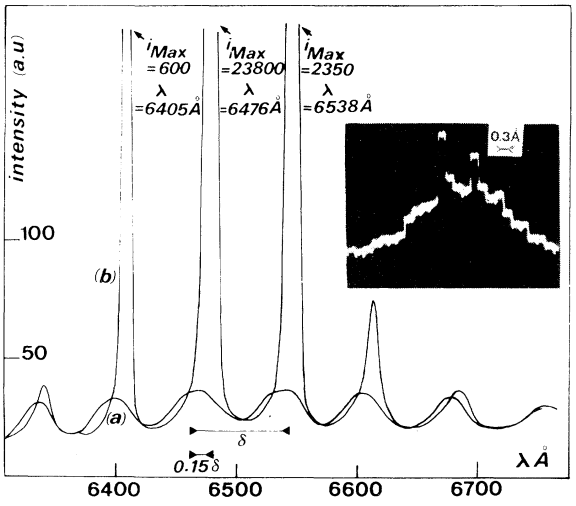

FIG. 4. Spectra of the cavity output radiation under two conditions: curve *a*, cavity detuned (no amplification) and curve *b*, cavity tuned (laser on).

power over the 1-ns electron bunch length (including effects of both the long- and short-time-scale pulse structure of the laser), and a 2-kW intracavity peak power. 75 μW give a 2.4×10^{-5} efficiency with respect to the 3.1 W of total synchrotron radiation power generated in the whole storage ring at this energy and current. This efficiency is about 0.4 the Renieri typical efficiency[7]

$$\eta = (\sigma_E/E)\eta_{\mathrm{mir}},$$

where

$$\eta_{\mathrm{mir}} = \frac{\text{mirror transmission}}{\text{round trip cavity losses}}$$

and $\sigma_E/E = 1.2\times10^{-3}$ is the RMS relative energy spread. In this experiment $\eta_{\mathrm{mir}} = 0.043$. This low mirror efficiency is mainly due to the high absorption in the mirror dielectric compared to its transmission. The rather low Renieri average output power is therefore the result of high sensitivity of the OK to energy spread, poor mirror efficiency, and weak total synchrotron radiation power at 166 MeV (power is proportional to the fourth power of the electron energy). The laser output power always decreases with the electron beam current and, except in regions too close to threshold, is usually proportional to the current as predicted by the same model. However, important discrepancies appear in the structure for long time scales (see Fig. 3) which is predicted to be constant. Moreover, bunch shortening instead of bunch lengthening has been seen at laser turnon; such an effect has already been seen at much lower current by simulating the FEL with an argon laser.[8]

In summary, this work demonstrates for the first time the feasibility of the storage-ring free-electron laser. Future experiments will continue to analyze the saturation mechanism, and the long- and short-time-scale structure. Higher gain/loss ratios are expected from the use of better mirrors, a second rf cavity, and smaller beam transverse dimensions obtained by using positrons instead of electrons.

This work was supported by the Direction des Recherches Etudes et Techniques under Contract No. 81/131 and by the U. S. Air Force Office of Scientific Research under Contract No. F 49620-80-C-0068.

The authors are greatly indebted to Yves Farge who initiated this research and to the technical support staff of the Laboratoire pour l'Utilisation du Rayonnement Electromagnétique for their invaluable help. Also, they thank the storage-ring staff of the Laboratoire de l'Accelerateur Lineaire, Orsay, for many fruitful discussions and the "Service Aimant" of the Laboratoire de l'Accelerateur Lineaire, Orsay, for experimental assistance.

[a]Permanent address: Ecole Supérieure de Physique et Chimie, 10 rue Vauquelin, F-75231 Paris Cedex 05, France.

[b]Permanent address: Département de Physico-Chimie, Service de Photophysique, Centre d'Etudes Nucléaires de Saclay, F-91191 Gif-sur-Yvette, France.

[c]Permanent address: Laboratoire de Photophysique Moléculaire, Bâtiment 213, Université de Paris-Sud, F-91405 Orsay, France.

[d]Permanent address: Deacon Research, 754 Duncardine Way, Sunnyvale, Cal. 94087.

[1]D. A. G. Deacon, L. R. Elias, J. M. J. Madey, G. J. Ramian, H. A. Schwettman, and T. I. Smith, Phys. Rev. Lett. 38, 892 (1977).

[2]J. M. Ortega, C. Bazin, D. A. G. Deacon, C. Depautex, and P. Elleaume, Nucl. Instrum. Methods 206, 281 (1983).

[3]M. Billardon, D. A. G. Deacon, P. Elleaume, J. M. Ortega, K. E. Robinson, C. Bazin, M. Bergher, J. M. J. Madey, Y. Petroff, and M. Velghe, J. Phys. (Paris), Colloq. 44, C1-29 (1983).

[4]N. A. Vinokurov and A. N. Skrinsky, Institute of Nuclear Physics, Novosibirsk, Report No. INP 77-59, 1977 (unpublished); see also N. A. Vinokurov, in *Proceedings of the Tenth International Conference on High Energy Charged Particle Accelerators, Serpukhov, 1977* (Institute Siziki Zysokikh Energie, Serpukhov, U.S.S.R., 1977), Vol. 2, p. 454.

[5]P. Elleaume, J. Phys. (Paris), Colloq. 44, C1-333 (1983). See also P. Elleaume, *Physics of Quantum Electronics* (Addison-Wesley, Reading, Mass., 1982), Vol. 8, Chap. 5, p. 119.

[6]J. M. J. Madey, Nuovo Cimento B50, 64 (1979).

[7]A. Renieri, Nuovo Cimento B53, 160 (1979); G. Dattoli and A. Renieri, Nuovo Cimento B59, 1 (1980).

[8]K. E. Robinson, D. A. G. Deacon, M. F. Velghe, and J. M. J. Madey, IEEE J. Quantum Electron. 19, 365 (1983).

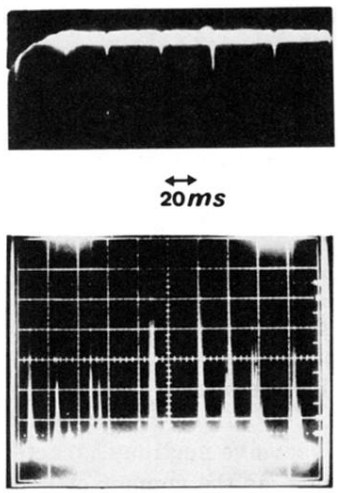

FIG. 3. Laser time structure over a 200-ms interval. Curve *b* is recorded in the same condition as *a*, but with a higher detector sensitivity.

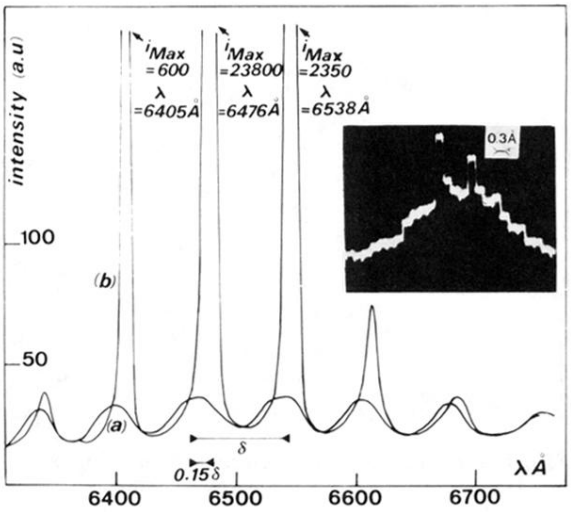

FIG. 4. Spectra of the cavity output radiation under two conditions: curve *a*, cavity detuned (no amplification) and curve *b*, cavity tuned (laser on).